Properties of self-assembled Bi nanolines on InAs(100) studied by core-level and valence-band photoemission, and first-principles calculations

M. Ahola-Tuomi,[1,*] M. P. J. Punkkinen,[1,2] P. Laukkanen,[1,3] M. Kuzmin,[1,4] J. Lång,[1] K. Schulte,[5]
A. Pietzsch,[5] R. E. Perälä,[1] N. Räsänen,[1] and I. J. Väyrynen[1]

[1]*Department of Physics and Astronomy, University of Turku, FI-20014 Turku, Finland*
[2]*Applied Materials Physics, Department of Materials Science and Engineering, Royal Institute of Technology, SE-10044 Stockholm, Sweden*
[3]*Optoelectronics Research Centre, Tampere University of Technology, FI-33101 Tampere, Finland*
[4]*Ioffe Physico-Technical institute, Russian Academy of Sciences, St. Petersburg 194021, Russian Federation*
[5]*MAX-lab, Lund University, SE-22100 Lund, Sweden*
(Received 24 March 2011; published 8 June 2011)

We have studied self-assembled bismuth (Bi) nanolines on the Bi-terminated InAs(100) surface by core-level and valence-band photoelectron spectroscopy, and *ab initio* first-principles calculations. A structural model for this intriguing surface is suggested based on the comparison of the measured and calculated core-level shifts. Also, the atomic origins for the core-level shifts are proposed based on the calculations. A clear peak related to this surface was observed in the valence band 0.34 eV below the Fermi level, which can be used as a "fingerprint" of a well-ordered Bi/InAs(100) nanoline surface.

I. INTRODUCTION

The study of well-defined single-crystal surfaces provides an opportunity to reveal the fundamental mechanisms behind several phenomena that occur on surfaces, such as chemical reactions and catalysis, epitaxial growth of thin films, and self-assembly of nanostructures, which are all of great scientific importance. From the technological point of view, formation of periodically ordered nanostructures offers a possibility to fabricate prototype electronic devices based on the quantum confinement of electron states.[1–5] Semiconductor surfaces are particularly interesting in this aspect since the surface states inside the gap cannot couple with the substrate.[1] Furthermore, different nanostructures can be used as templates to grow other ordered nanoscale systems with electronic, optical, or even magnetic properties, which may differ drastically from those of a bulk system.[6–8]

In particular, a number of studies, both experimental and theoretical, have been performed on self-assembled one-dimensional (1D) systems such as nanowires and nanolines.[6–16] For example, stepped silicon surfaces have been used to orient different metals and molecules,[5,6,14] silicon quantum wires have been grown on Ag(110),[11,12] and various metals (Pt, In, Pb, etc.) form atomic lines on the Ge- or Si(100)(2 × 1) substrates.[16,17] Also, one of the most studied systems is the Si(100)(2 × 1) surface with highly ordered Bi nanolines, which consist of two parallel rows of symmetric Bi dimers.[7–10] Besides the fundamental studies of exotic behavior of quantized electronic states and charge transport, such structures could be used, for example, as interconnections in nanoelectronics or as a one-dimensional grating in the molecular scale.[7,18] Significantly fewer studies have been reported on 1D systems on III-V(100) semiconductor surfaces, which is surprising considering their technological importance. Also, their surface structures are inherently single domain, which is an important feature when studying, for example, the transport properties of surfaces. On the other hand, Bi is an interesting material since its stepped surfaces have 1D spin-split surface states, which could be used as spin selectors in electronic devices (i.e., spintronics).[19]

We have found that by self-assembly, it is possible to produce a uniform, large-scale, single-domain pattern of Bi nanolines on the InAs(100) substrate.[20] The first monolayer (ML) of Bi grows two dimensionally producing a (2 × 1) structure in which the Bi atoms form dimers in the [0$\bar{1}$1] direction. On top of this Bi/InAs(100)(2 × 1) surface, the second layer grows into one-dimensional Bi chains, which are aligned parallel to each other by additional heating after the Bi deposition. Based on our STM (scanning tunneling microscopy) and LEED (low-energy electron diffraction) studies, we concluded that the lines are 4.3 nm apart and have a double periodicity along the line indicating that the lines are formed by Bi dimers parallel to the dimers of the underlying (2 × 1) structure. This corresponds to a (2 × 10) reconstruction of the Bi/InAs(100) surface. Density-functional calculations of AlZahrani and Srivastava supported this tentative atomic model.[21] However, the understanding of the atomic and electronic structure of the Bi/InAs(100) nanoline surface is far from complete due to the limited number of measurements reported on this surface, and we address this issue by reporting core-level and valence-band photoemission data complementary to previous STM and LEED studies, which provide important criteria for building up the atomic model for this surface. Also, a number of new atomic models are considered by theoretical calculations.

In this study, we monitored the formation of the Bi nanolines on the Bi/InAs(100)(2 × 1) substrate and their removal by core-level and valence-band photoemission. The experimental results were combined with first-principles calculations, because especially the comparison of the measured and calculated core-level shifts provides detailed structural information,[22] although the size of the (2 × 10) unit cell represents a significant challenge for the calculations. The core-level photoemission results which are supported by the calculations show two new surface core-level shift components for the Bi 5*d* photoemission spectra from the surface with

Bi nanolines compared to the Bi/InAs(100)(2 × 1) substrate. This indicates that the nanolines are indeed induced by Bi. According to the calculations, Bi dimers of the actual lines, Bi dimers on both sides of the lines, and Bi dimers underneath the lines contribute to those shifts. Photoemission intensity at the Fermi level suggests that the surface is slightly metallic. Furthermore, a clear peak was observed at 0.34 eV below the Fermi level for the well-ordered Bi-nanoline surface. Interestingly, the peak arises from the (2 × 1)-Bi areas between the nanolines according to the calculations. However, the presence of the Bi nanolines clearly enhances the emission. Finally, we propose an atomic model hitherto not reported for the Bi/InAs(100) nanoline surface, which is energetically favored and explains all the experimental data up to date.

II. EXPERIMENTAL DETAILS

The photoemission experiments were performed at the Swedish Synchrotron Radiation Center MAX-lab on beamlines 41 and I511. On the beamline 41 the incident angle of the light was 45° relative to the surface normal. A hemispherical analyzer with angular resolution of 2° was used to measure the spectra and the spectral resolution was 100–200 meV depending on the photon energy used. I511 is an undulator-based beamline equipped with a Scienta SES-200 hemispherical electron analyzer. Grazing incidence of light (approximately 80° off surface normal) was used to measure the core-level spectra and the photon resolution of the photoelectron spectra was 30 meV. Both systems are equipped with LEED and Ar+ sputter gun and have a possibility for indirect sample heating. All spectra were recorded at room temperature.

InAs(100) substrates were cut from a S-doped (*n*-type) wafer. Cycles of 1-keV Ar ion sputtering with sample kept at 380°C and subsequent annealing at 470°C were used to clean the sample. Two or three cycles were needed to produce a sharp LEED pattern typical for the well-ordered In-rich InAs(100)c(8 × 2) surface [Fig. 1(a)].[23,24] Also, no indium oxide was observed in the In 4d core-level spectrum. On the beamline I511, no oxygen and carbon were detected by photoemission. Approximately 1.5 monolayers (MLs) of Bi was evaporated from a piece of Bi metal wrapped in a tungsten coil filament and the InAs(100) substrate was kept at room temperature during the evaporation. After the deposition, extra Bi was desorbed from the surface by additional heating at 250 °C. The Bi/InAs surface was then heated gradually and Bi 5d, In 4d, and As 3d core levels and the valence band were measured after each heating step. The experiments were performed more thoroughly on the beamline 41 at MAX I, and some of the measurements were repeated on the beamline I511 at MAX II, which accounts for the different experimental resolution in the resulting spectra. Photon energies for the photoemission measurements were chosen considering the surface sensitivity and resolution. In both systems, the Fermi level was measured on a cleaned Ta plate, which was mounted to the sample holder in electrical contact with the sample. Temperature was monitored by an infrared pyrometer.
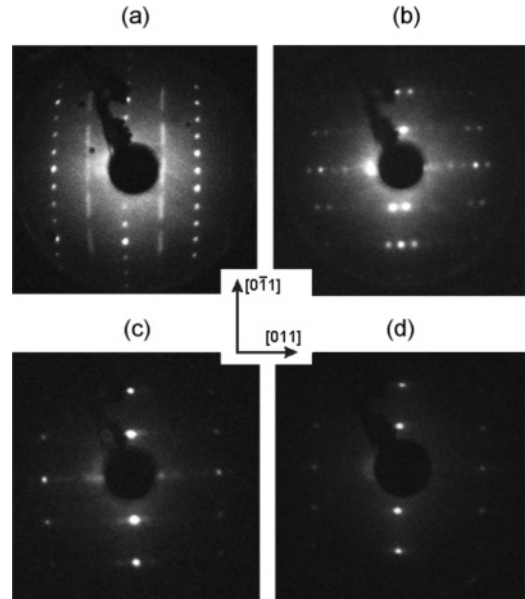
FIG. 1. (a) LEED pattern of the clean InAs(100)c(8 × 2) (55 eV), (b) Bi/InAs(100)(2 × 6) (44 eV), (c) Bi/InAs(100)(2 × 1) with Bi nanolines [i.e., (2 × 10)] (42 eV), and (d) Bi/InAs(100)(2 × 1) surface (43 eV).

III. CALCULATIONS

Theoretical calculations were performed using the *ab initio* density-functional total-energy code with the local-density approximation (LDA).[25,26] The approach is based on plane-wave basis and projector augmented wave method[27,28] (Vienna *ab initio* simulation package, VASP)[29–32] The calculations were performed using (2 × 10) slabs, including 13 atomic layers (+ pseudohydrogen atoms) and treating the d electrons as core electrons. The dangling bonds of the bottom surface As atoms were passivated by pseudohydrogen atoms ($Z = 0.75$). A theoretical LDA lattice constant (4.28 Å) was used, and two bottom atomic layers of the slabs were fixed to the ideal bulk positions. Other atoms, including the pseudohydrogen atoms, were relaxed using conjugate-gradient minimization of total energy until the remaining forces were less than 30 meV/Å. The energy cutoff was 300 eV. The number of k points in the surface Brillouin zone was 10. The k-point sampling was performed by the Monkhorst-Pack scheme with the origin shifted to the Γ point.[33] Surface core-level shifts (SCLSs) were calculated within the initial-state model.[22]

IV. RESULTS AND DISCUSSION

A. LEED

A (2 × 6)/c(2 × 12)] LEED pattern was observed straight after Bi deposition [Fig. 1(b)]. A similar LEED pattern has also been observed for the Bi-induced InAs(100) surface previously with similar coverage.[34,35] In our experiments, we observed a clear (2 × 6) structure for a number of coverages from 1 ML up to 3 MLs even *without* annealing, which indicates that the surface has a periodic structure. However, this (2 × 6) pattern does not correspond to an ordered reconstruction, but rather an average over the surface with "meandering" lines.[20] On top of these lines, Bi islands start to form with
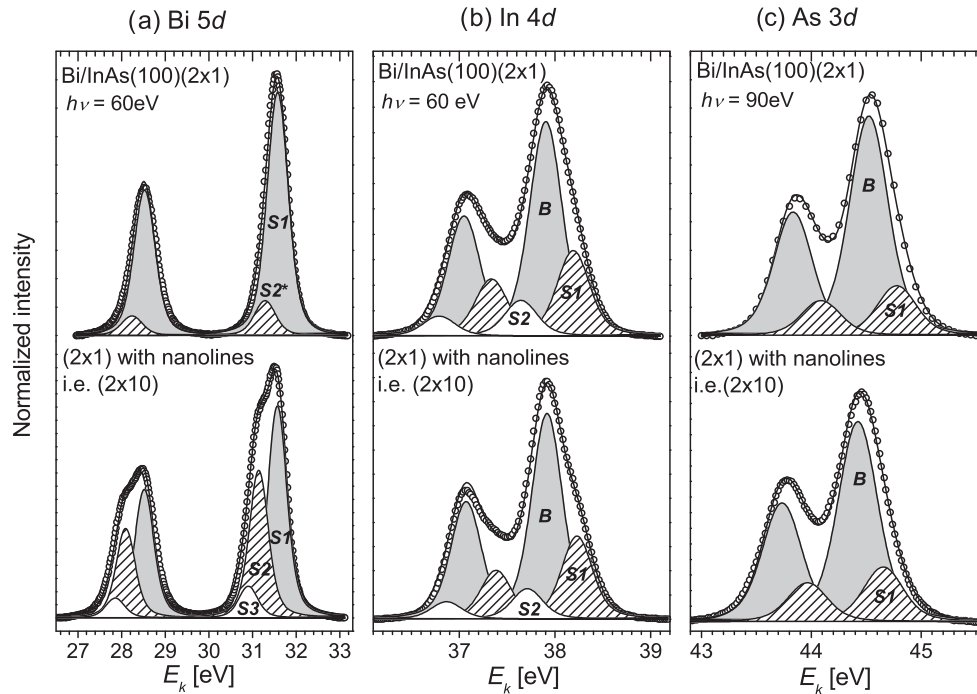
FIG. 2. Comparison of the Bi $5d$, In $4d$, and As $3d$ core-level photoelectron spectra from the Bi/InAs(100)(2 × 1) surface and the same surface with Bi nanolines [i.e., Bi/InAs(100)(2 × 10)]. The spectra were measured on beamline I511 at Max II.

increasing Bi coverage, which gives a faint (1 × 1) LEED pattern co-existing with the (2 × 6)/c(2 × 12), which was also verified with STM (not shown here). After heating the sample at 250 °C for several hours, the (2 × 6) changed to a (2 × 1) with elongated or some additional, nonresolvable spots in the [011] direction [Fig. 1(c)]. Similar streaking of the substrate spots has been observed for the Si/Ag(110) surface with self-aligned Si nanowires.[12] After heating at 280 °C, the streaking of the LEED spots disappeared and the pattern changed to a (2 × 1) with no additional spots [Fig. 1(d)].[36] Heating at 450 °C for approximately 30 min removed Bi completely, restoring the c(8 × 2) pattern of the clean surface.

B. Core-level spectroscopy

The core-level spectra from Bi $5d$, In $4d$, and As $3d$ levels of the Bi/InAs(100)(2 × 1) surface and the same surface with Bi nanolines are presented in Fig. 2. All the spectra were measured at beamline I511. The double-peak line shapes are caused by spin-orbit splitting of the d levels into the $d_{3/2}$ and $d_{5/2}$ components. Because the atoms in the surface and bulk have different chemical environments, small shifts in binding energies are observed when measuring core-level photoemission. These differences are called surface core-level shifts, which give information of the atomic arrangement of a surface. The core-level shift components resulting from the fitting are marked as S. Voigt line shape was used in the fitting process of the core-level spectra,[37] and the background was removed by Shirleys method.[38] Lorenzian widths of 0.16, 0.16, and 0.20 eV and the spin-orbit splitting of 0.855, 0.69, and 3.05 eV were used for In $4d$, As $3d$, and Bi $5d$ spectra, respectively, in agreement with previous studies.[34,39,40] The

branching ratio of the $d_{5/2}$ and $d_{3/2}$ components was allowed to vary slightly from its statistical value of 1.5 because of the possible diffraction effects.[41,42] For the spectra measured on the beamline 41 (I511), the Gaussian width of 0.45 (0.31) eV was used for the As $3d$ spectra, which was deducted from the spectra with only a bulk component. Gaussian widths of 0.41 (0.29) and 0.51 (0.40) eV were used for In $4d$ and Bi $5d$, which resulted from the fitting of the spectra with a minimum number of components. Similar values for the Gaussian widths have also been used before.[34,35,39,43]

First we consider the spectra from the surface without the lines, i.e., the Bi/InAs(100)(2 × 1). Although the discussion of the core-level shifts of the Bi/InAs(100) nanoline surface in context of the clean InAs(100)c(8 × 2) shifts might be useful, we find it misleading since the atomic structures of the clean and Bi-induced InAs(100) surface reconstructions are very different, and thus their core-level shifts are not well comparable. (Note that we have analyzed the clean InAs(100)c(8 × 2) reconstruction elsewhere.[44]) We have also previously studied several other Bi-induced III-V(100)(2 × 1) surfaces,[36,45] and we utilize those results in combination with our recent theoretical calculations to analyze the spectra here. The In $4d$ emission consists of three components marked B (bulk component), $S1$ on the 0.32-eV higher kinetic energy (lower binding energy) side of B, and $S2$ on the 0.18-eV lower kinetic energy (higher binding energy) side of B. $S1$ is assigned to the In atoms bonding to the Bi layer.[36,46] For the As $3d$ spectra, component $S1$ is found on the 0.25-eV higher kinetic energy side of B. This originates from the As atoms of the third surface layer. The origin of $S2$ in the In $4d$ spectra is discussed in the following.

The Bi $5d$ spectrum of the Bi/InAs(100)(2 × 1) surface consists of two SCLS components denoted as $S1$ and $S2^*$.

No bulk component exists because Bi is present only in the overlayer structure. According to our calculations, the most stable atomic model for this (2×1) surface consists of one ML of Bi with symmetric Bi-Bi dimers (called BiBi in our previous studies).[36,46] The structure of this (2×1) reconstruction is shown for the second Bi layer in the schematic image of the possible atomic structures for the nanoline surface in Fig. 4.[36] The component $S1$ in the Bi $5d$ emission is assigned to these Bi dimers. Some areas of the surface may contain a slightly different (2×1) phase depending on the surface preparation, which can effect the surface reconstruction.[36] Thus the origin of the small component $S2^*$ in the Bi $5d$ spectra on 0.30-eV lower kinetic energy compared to $S1$ is most likely due to another (2×1) phase(s) co-existing with the BiBi structure. The same explanation also applies to the $S2$ in the In $4d$ spectra. Also, some broadening of the In $4d$ spectra can be expected for the Bi/InAs(100)(2×1) surface compared to the nanoline surface. Since the nanoline surface contains more Bi than the (2×1) surface, it is thus mostly covered with the (2×1) BiBi phase whereas the Bi/InAs(100)(2×1) has more likely other phase(s) which broadens the spectral features.[36]

The comparison of the core-level spectra measured from the surface with Bi nanolines and the surface without the lines, i.e., the Bi/InAs(100)(2×1), shows that there are notable changes only in the core-level shifts of the Bi $5d$ emission. This gives us further support that the nanolines are made of Bi. Two new components, $S2$ and $S3$ on 0.43-eV and 0.69-eV lower kinetic energy side of $S1$, respectively, are found for the nanoline surface [i.e., Bi/InAs(2×10)]. Since $S2$ is on lower kinetic energy and it is much more intense than $S2^*$, it certainly represents a new core-level shift component, suggesting that the Bi on top of the (2×1) contributes to $S2$. We would like to note here that because of the experimental resolution, we cannot say whether $S2^*$ still exist, and contributes to the $S2$ emission also. However, in this case the contribution would be small and thus insignificant. Another component, $S3$, is found for the nanoline surface, which disappears as the lines are removed from the surface. This is therefore most likely related to the lines as well. Compared to the (2×1) substrate, new bonding sites are found for the nanoline surface: the Bi dimers forming the lines, the Bi atoms straight underneath the lines, and the Bi dimers on the sides of the lines. These all contribute to the Bi $5d$ emission, and will be discussed more closely in the next chapter. A comparison of the Bi $5d_{5/2}$ peak from the Bi/InAs(100) surface with different Bi coverage measured on the beamline 41 (with lower resolution than on I511) is shown in Fig. 3 to appoint the changes in the Bi $5d$ spectra as a function of Bi coverage. The excess Bi on top of the nanoline surface contributes to the component $S2$ which is seen from the bottom spectrum. This is reasonable, since the binding environment is similar as for the dimers in the lines since all the Bi dimers on the top layer are bonded to Bi.

The Bi $5d_{5/2}$ spectra from the nanoline surface [i.e., the (2×10)], measured on beamline I511 with better resolution than the previous Bi $5d_{5/2}$ spectra, is presented in Fig. 5. Three surface core-levels shift components were found in the fitting procedure. The positions of $S2$ (0.43 eV) and $S3$ (0.69 eV) refer to the $S1$, which is assigned to the Bi dimers
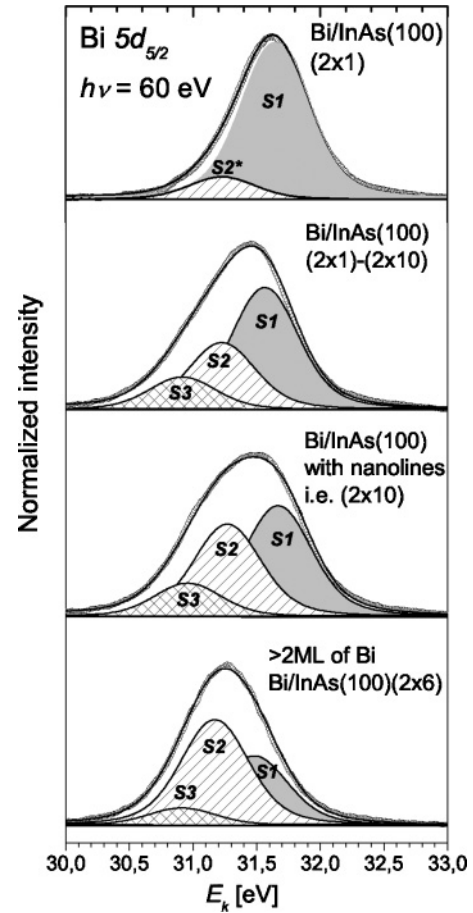
FIG. 3. Bi $5d_{5/2}$ spectra measured from the Bi/InAs(100) with different Bi coverage (i.e., different surface reconstruction) on the beamline 41 at MAX I.

of the Bi/InAs(100)(2×1) BiBi structure, as previously stated. We have examined several possible models for the atomic structure of the Bi nanolines, and our total-energy calculations show that the most stable structures consist of Bi dimers parallel to the dimers of the (2×1) as shown in Figs. 4(a)–4(d). This is in agreement with a very recent theoretical study by AlZahrani *et al.*,[21] who also concluded that the Bi/InAs(100) nanoline surface has parallel Bi dimers on top of the (2×1) substrate. However, we also considered some new atomic models compared to the previous studies, and we found energetically more stable structures. The results for the corresponding surface energies of the models are also shown in Fig. 4. The lowest surface energy was found for the models (d) and (h) in Fig. 4, which both were 0.031 eV/ [(1×1) unit-cell area] lower than the surface energy of (a), which was considered as the most stable model in the previous study.[21]

Since the calculated surface energy differences for the most stable atomic models [Figs. 4(a)–4(d) and 4(h)] were relatively small [within 0.03 eV/(1×1) area], the core-level shifts for these models were calculated. They are presented in Table I. According to the calculations for models [(a)–(d)] in Fig. 4, three surface core-level shifts are present in the Bi $5d$ emission besides the component from the Bi dimers of the (2×1) structure. By comparing
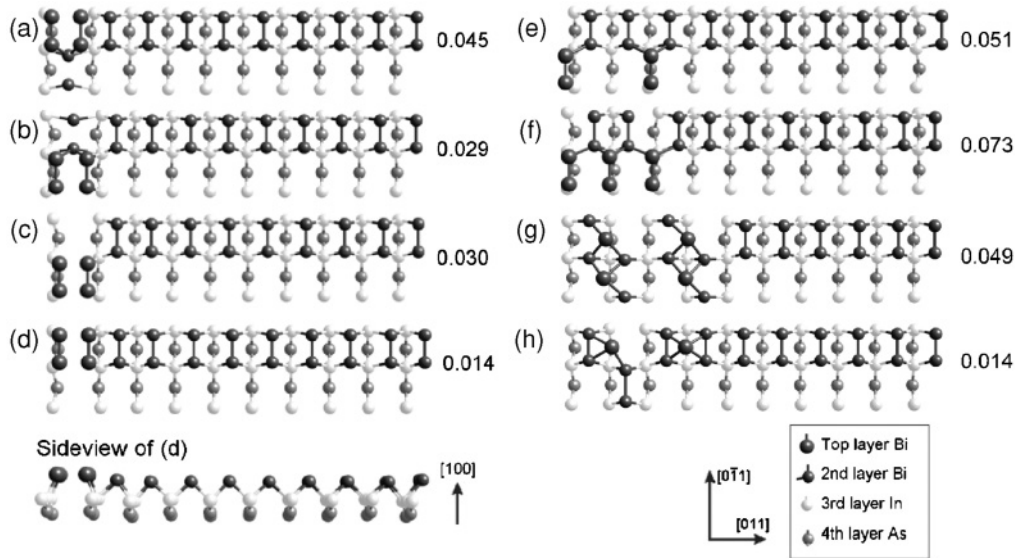
FIG. 4. (a)–(h) Schematic drawings (top view) of some atomic models and their surface energies [in units of eV/(1×1) area] considered for the Bi/InAs(100) surface with Bi nanolines. The energies refer to the surface energy of the Bi/InAs(100)(2×1) substrate.

the measured and calculated core-level shifts, we can confidently rule out model (c) in Fig. 4. Also, even though model (h) has the lowest energy besides model (d), the calculated core-level shifts are in contradiction with the measured ones. Furthermore, the calculated STM image of model (h) in Fig. 6(c) does not correspond well to the measured one in Fig. 6. However, one cannot distinguish whether the calculated STM image in Figs. 6(a) or 6(b) describes the measured STM image better. Thus we do not consider the atomic model (h) in Fig. 4 further either. When considering models (a) and (b) in Fig. 4, the component on energy position +0.37 and [+0.33] eV arises from the Bi dimers of the (2×1) structure on both sides of the lines. The component on position +0.60 [+0.64] arises from the Bi dimers in the actual lines, and the one on the highest binding energy, +0.82 [+0.87], is assigned to the Bi atoms straight underneath these lines. The same explanation also applies to the components on energy positions +0.42 (dimers on the side of the lines), and +0.48 (dimers on the lines) for model (d), but the component at the position +0.59 is assigned to the dimers of the (2×1)

TABLE I. Measured and calculated core-level shifts for different Bi nanoline structures on Bi/InAs(100)(2×1). All these nanoline structures have dimers parallel to the substrate 2×1 dimers. Positive energy corresponds to larger binding energy (smaller kinetic energy) referred to by the binding energy of the BiBi dimers of the Bi/InAs-(2×1) substrate ($S1$ at 0 eV). Values are in eV.

Measured Bi $5d$ SCLS:	0,	+0.43,	+0.69	
Calculated shifts (VASP):				
model (a)	0	+0.37	+0.60	+0.82
model (b)	0	+0.33	+0.64	+0.87
model (c)	0	−0.12	+0.01	+0.10
model (d)	0	+0.42	+0.48	+0.59
model (h)	0	−0.16, +0.13	+0.24	+0.35, +0.39

structure, which sit *next* to the dimers on the side of the lines [Fig. 4(d)] since the dimers underneath the lines are missing.

By keeping in mind that the strength of the theory is to reveal the number of the core-level shifts and their atomic origins but not necessary to give the very exact values for the energy positions of the components,[46] the agreement is excellent when considering the limitations of the experimental resolution, which prevents the separation of the smaller energy shifts. Thus we conclude that two atomic positions contribute to $S2$ in Fig. 5: the Bi dimers on both sides of the lines and the Bi dimers on the lines. $S3$ in Fig. 5 arises from the Bi atoms underneath the lines [models (a) and (b) in Fig. 4] *or* from the Bi dimers next to the Bi dimers on the sides of the lines [model (d) in Fig. 4]. Also, the relative intensities of $S1$, $S2$, and $S3$ support the previous interpretation. As mentioned above, model (d) in Fig. 4 has the lowest surface energy and therefore

FIG. 5. Bi $5d_{5/2}$ from the Bi/InAs(100) surface with Bi nanolines measured at MAX II, beamline I511. Three surface core-level shifts, $S1$, $S2$, and $S3$, are present.
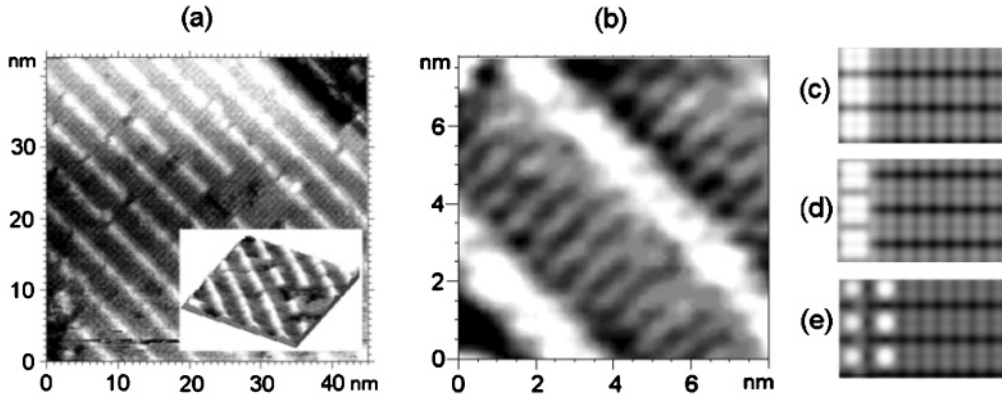
FIG. 6. (a) Large-scale STM image of the Bi nanolines on the InAs(100) surface. The inset is from the same image in 3D display. (b) An empty-states STM image ($V = 2.2$ V, $I = 0.4$ nA) of the surface. (c)–(e) Calculated images of three different models: (d), (b), and (h) in Fig. 4, respectively, with the same bias as the measured one.

it is the most stable structure according to our calculations. Furthermore, the agreement between the calculated and the measured core-level shifts is better for model (d) than for the other two models, (a) and (b) in Fig. 4. Thus we conclude that the Bi nanolines are made of dimers parallel to the Bi dimers of the Bi/InAs(100)(2 × 1) structure, and suggest that the schematic atomic model (d) with 1.1 MLs of Bi in Fig. 4 has the closest resemblance to the Bi/InAs(100) nanoline surface of all the studied ones to date.

C. Valence-band spectroscopy

The valence-band spectra referred to by the Fermi level (E_f) before and after deposition with increasing Bi coverage from the bottom to the top spectrum (i.e., with different surface reconstruction) are presented in Fig. 7. All the valence-band spectra were measured on beamline 41 at Max I with normal emission. The photon energy of 30 eV was chosen, since below
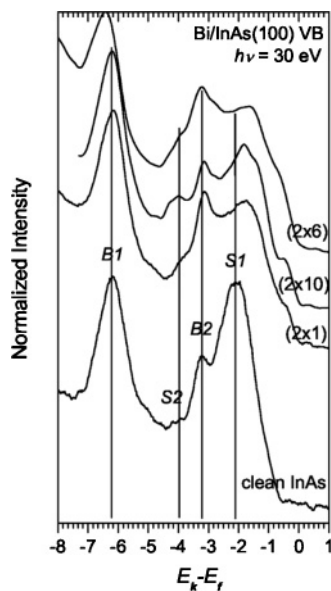
FIG. 7. Valence band of the InAs(100) surface with different Bi coverage (i.e., different surface reconstruction). The spectra were measured on beamline 41 at MAX I.

this energy the Bi 5d emission excited by the second-order light overlaps the valence spectra. On the valence spectrum of the clean InAs(100)(4 × 2) surface, peaks marked $B1$ and $B2$ are related to the bulk interband transitions.[47] These are also present in the spectra after the Bi deposition. The intensity of a peak marked $S1$ at binding energy around 2 eV decreases clearly after the Bi deposition. The peak at the same binding energy marked $B1$ (or S_{res} in previous studies) was identified as a surface resonance present only on the clean In-rich InAs(100)(4 × 2) but not on the As-rich (2 × 4) surface.[47,48] Our observation agrees with this since Bi deposition destroys the surface (4 × 2) reconstruction. Also, $S2$ was previously identified as a surface feature, arising either from the backbonds or the dimer bonds of the surface dimers.[47,49] The same feature is also present on the Bi terminated surface, which suggests that it originates from the backbonds of the In atoms of the third surface layer, since the dimer bonds of the surface In (or As) dimers break as a consequence of Bi deposition. Similar assumption was also made by Szamota-Leandersson *et al.*[35] The most interesting changes occur in the top of the valence band, presented in Fig. 8.

On the clean surface, E_f is located 0.45 eV above the valence-band maximum (VBM). The position of the VBM was determined by the analysis of the In 4d emission and the In 4d–VBM separation.[50,51] Since the InAs band gap is 0.36 eV, downward band bending of about 0.1 eV is observed for the clean InAs(100)(4 × 2). This agrees with previous studies,[50,52] where pinning of the surface E_f was found to be 0.1 eV or close to the conduction-band minimum (CBM), respectively. However, stronger band bending has also been found for this surface.[24,35] Therefore the E_f pinning seems to depend on the preparation conditions or the surface quality.[53] Also, it may be of interest to note here that for the molecular-beam epitaxy grown samples the E_f was found 0.02 eV below the CBM for the clean In-terminated InAs(100)(4 × 2).[47] For the nanoline surface and the same surface without the lines, i.e., Bi/InAs(100)(2 × 1), the E_f-VBM separation was found to be similar to for the clean surface, 0.41–0.43 eV. For more disoriented surfaces (Bi amount of 2–3 MLs), E_f was observed to move further above the CBM. Also, slight emission at the E_f is observed for these Bi-terminated surfaces, indicating a
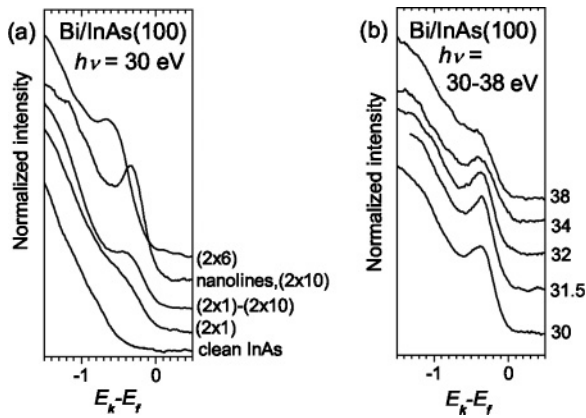
FIG. 8. (a) Top of the valence band measured from the Bi/InAs(100) surface with different Bi coverage. (b) Top of the valence band from the Bi/InAs(100) nanoline surface measured with different photon energy. The spectra were measured on beamline 41 at MAX I.

metallic (or semimetallic) surface. The metallicity is enhanced for higher Bi coverage, which agrees with the pinning of the E_f well above the CBM.

The top of the valence band of the Bi/InAs(100) with increasing Bi coverage from the bottom to the top spectrum is presented more closely in Fig. 8(a). For the surface with 1.1 MLs of Bi, i.e., the Bi/InAs(100)(2×1) with Bi nanolines, a clear peak arises with the binding energy of 0.34 eV. No energy dispersion is observed for this peak, as seen in Fig. 8(b). Figures 7 and 8 show that the emission at 0.34 eV enhances for the (2×10) surface with the most ordered Bi lines. The calculations reveal that this emission originates from the (2×1)-Bi areas between the top layer lines of the Bi-nanoline (2×10) surface, being reasonable because a similar emission appears also on the pure (2×1)-Bi reconstruction. However, it is interesting that the presence of the Bi nanolines clearly improves the 0.34-eV emission suggesting a resonance-type behavior behind it. Future investigations are needed to clarify that. The same peak is not found for the surface with 2 MLs of Bi, which indicates that the second surface layer is not so well

oriented. However, a bump with slightly higher binding energy is present. Previously, a state in the valence band with similar binding energy (0.6 eV) was observed for the Bi/InAs(100) with 3.5 MLs of Bi,[35] which was attributed to the topmost occupied Bi dangling bonds. This also applies here.

V. CONCLUSIONS

In conclusion, based on the comparison of the measured and calculated core-level shifts and the calculated surface *ab initio* energies, we have proposed a new atomic model with 1.1 MLs of Bi for the interesting self-assembled Bi nanolines with (2×10) periodicity on the InAs(100) surface. This model agrees with the previous STM measurements. Furthermore, we have observed the enhanced valence-band emission at 0.34 eV below the Fermi level on the well-ordered Bi-nanoline surface, which interestingly arises from the (2×1)-Bi areas between the nanolines, as the calculations demonstrate. This can be used as a fingerprint of a well-ordered surface. The presented results give further assistance to the understanding of the formation mechanisms behind the self-assembled Bi nanolines.

*marahola@utu.fi

[1] F. J. Himpsel, K. N. Altmann, J. N. Crain, A. Kirakosian, J.-L. Lin, A. Liebsch, and V. P. Zhukov, J. Electron Spectrosc. Relat. Phenom. **126**, 89 (2002).

[2] Xiangdong Liu, Bin Lu, Takushi Iimori, Kan Nakatsuji, and Fumio Komori, Phys. Rev. Lett. **98**, 066103 (2007).

[3] H. W. Yeom, S. Takeda, E. Rotenberg, I. Matsuda, K. Horikoshi, J. Schäfer, C. M. Lee, S. D. Kevan, T. Ohta, T. Nagao, and S. Hasegawa, Phys. Rev. Lett. **82**, 4898 (1999).

[4] V. A. Shchukin and D. Bimberg, Rev. Mod. Phys. **71**, 1125 (1999).

[5] H. W. Yeom, Y. K. Kim, E. Y. Lee, K.-D. Ryang, and P. G. Kang, Phys. Rev. Lett. **95**, 205504 (2005).

[6] P. Segovia, D. Purdie, and M. Hengsberger, Nature (London) **402**, 504 (1999).

[7] R. V. Belosludov, A. A. Farajian, H. Mizuseki, K. Miki, and Y. Kawazoe, Phys. Rev. B **75**, 113411 (2007).

[8] W. Orellana and R. H. Miwa, Appl. Phys. Lett. **89**, 093105 (2006).

[9] J.-T. Wang, E. G. Wang, D. S. Wang, H. Mizuseki, Y. Kawazoe, M. Naitoh, and S. Nishigaki, Phys. Rev. Lett. **94**, 226103 (2005).

[10] R. H. Miwa, J. M. MacLeod, G. P. Srivastava, and A. B. McLean, Appl. Surf. Sci. **244**, 157 (2005).

[11] P. De Padova, C. Quaresima, P. Perfetti, B. Olivieri, C. Leandri, B. Aufray, S. Vizzini, and G. Le Lay, Nano Lett. **8**, 271 (2008).

[12] M. A. Valbuena, J. Avila, M. E. Dávila, C. Leandri, B. Aufray, G. Le Lay, and M. C. Asensio, Appl. Surf. Sci. **254**, 50 (2007).

[13] P. De Padova, C. Leandri, S. Vizzini, C. Quaresima, P. Perfetti, B. Olivieri, H. Oughaddou, B. Aufray, and G. Le Lay, Nano Lett. **8**, 2299 (2008).

[14]F. J. Himpsel, J. L. McChesney, J. N. Crain, A. Kirakosian, V. Pérez-Dieste, Nicholas L. Abbott, Yan-Yeung Luk, Paul F. Nealey, and Dmitri Y. Petrovykh, J. Phys. Chem. B **108**, 14484 (2004).

[15]Feng Liu, J. Tersoff, and M. G. Lagally, Phys. Rev. Lett. **80**, 1268 (1998).

[16]Nuri Oncel, Arie van Houselt, Jeroen Huijben, Ann-Sofie Hallbäck, Oguzhan Gurlu, Harold J. W. Zandvliet, and Bene Poelsema, Phys. Rev. Lett. **95**, 116801 (2005).

[17]Z.-C. Dong, D. Fujita, and H. Nejoh, Phys. Rev. B **63**, 115402 (2001).

[18]H. Sahaf, L. Masson, C. Léandri, B. Aufray, G. Le Lay, and F. Ronci, Appl. Phys. Lett. **90**, 263110 (2007).

[19]Ph. Hofmann, Prog. Surf. Sci. **81**, 191 (2006).

[20]M. Ahola-Tuomi, P. Laukkanen, M. P. J. Punkkinen, R. E. Perälä, I. J. Väyrynen, M. Kuzmin, K. Schulte, and M. Pessa, Appl. Phys. Lett. **92**, 011926 (2008).

[21]A. Z. AlZahrani and G. P. Srivastava, J. Appl. Phys. **106**, 053713 (2009).

[22]M. P. J. Punkkinen, P. Laukkanen, K. Kokko, M. Ropo, M. Ahola-Tuomi, I. J. Väyrynen, H.-P. Komsa, T. T. Rantala, M. Pessa, M. Kuzmin, L. Vitos, J. Kollár, and B. Johansson, Phys. Rev. B **76**, 115334 (2007).

[23]C. Kendrick, G. LeLay, and A. Kahn, Phys. Rev. B **54**, 17877 (1996).

[24]P. De Padova, C. Quaresima, P. Perfetti, R. Larciprete, R. Brochier, C. Richter, V. Ilakovac, P. Bencok, C. Teodorescu, V. Y. Aristov, R. L. Johnson, and K. Hricovini, Surf. Sci. **482–485**, 587 (2001).

[25]D. M. Ceperley and B. J. Alder, Phys. Rev. Lett. **45**, 566 (1980).

[26]J. P. Perdew and A. Zunger, Phys. Rev. B **23**, 5048 (1981).

[27]P. E. Blöchl, Phys. Rev. B **50**, 17953 (1994).

[28]G. Kresse and D. Joubert, Phys. Rev. B **59**, 1758 (1999).

[29]G. Kresse and J. Hafner, Phys. Rev. B **47**, 558 (1993).

[30]G. Kresse and J. Hafner, Phys. Rev. B **49**, 14251 (1994).

[31]G. Kresse and J. Furthmüller, Comput. Mater. Sci. **6**, 15 (1996).

[32]G. Kresse and J. Furthmüller, Phys. Rev. B **54**, 11169 (1996).

[33]H. J. Monkhorst and J. D. Pack, Phys. Rev. B **13**, 5188 (1976).

[34]P. Laukkanen, M. Ahola, M. Kuzmin, R. E. Perälä, I. J. Väyrynen, and J. Sadowski, Surf. Sci. **598**, L361 (2005).

[35]K. Szamota-Leandersson, M. Leandersson, P. Palmgren, M. Göthlied, and U. O. Karlsson, Surf. Sci. **603**, 190 (2009).

[36]P. Laukkanen, M. P. J. Punkkinen, H.-P. Komsa, M. Ahola-Tuomi, K. Kokko, M. Kuzmin, J. Adell, J. Sadowski, R. E. Perälä, M. Ropo, T. T. Rantala, I. J. Väyrynen, M. Pessa, L. Vitos, J. Kollár, S. Mirbt, and B. Johansson, Phys. Rev. Lett. **100**, 086101 (2008).

[37]J. J. Joyce, M. Del Giudice, J. H. Weaver, J. Electron Spectrosc. Relat. Phenom. **49**, 31 (1989).

[38]D. A. Shirley, Phys. Rev. B **5**, 4709 (1972).

[39]M. Ahola-Tuomi, P. Laukkanen, R. E. Perälä, M. Kuzmin, J. Pakarinen, I. J. Väyrynen, and M. Adell, Surf. Sci. **600**, 2349 (2006).

[40]J. N. Andersen and U. O. Karlsson, Phys. Rev. B **41**, 3844 (1990).

[41]M. T. Sieger, T. Miller, and T.-C. Chiang, Phys. Rev. Lett. **75**, 2043 (1995).

[42]H. W. Yeom, T. Abukawaa, Y. Takakuwaa, S. Fujimorib, T. Okaneb, Y. Oguraa, T. Miurab, S. Satob, A. Kakizakic, and S. Konoa, Surf. Sci. **395**, L236 (1998).

[43]P. Palmgren, B. R. Priya, N. P. P. Niraj, and M. Göthelid, J. Phys.: Condens. Matter **18**, 10707 (2006).

[44]P. Laukkanen, M. P. J. Punkkinen, M. Ahola-Tuomi, J. Lång, K. Schulte, A. Pietzsch, M. Kuzmin, J. Sadowski, J. Adell, R. E. Perälä, M. Ropo, K. Kokko, L. Vitos, B. Johansson, M. Pessa, and I. J. Väyrynen, J. Electron Spectrosc. Relat. Phenom. **177**, 52 (2010).

[45]P. Laukkanen, J. Pakarinen, M. Ahola-Tuomi, M. Kuzmin, R. E. Perälä, I. J. Väyrynen, A. Tukiainen, J. Konttinen, P. Tuomisto, and M. Pessa, Phys. Rev. B **74**, 155302 (2006).

[46]M. P. J. Punkkinen, P. Laukkanen, H.-P. Komsa, M. Ahola-Tuomi, N. Räsänen, K. Kokko, M. Kuzmin, J. Adell, J. Sadowski, R. E. Perälä, M. Ropo, T. T. Rantala, I. J. Väyrynen, M. Pessa, L. Vitos, J. Kollár, S. Mirbt, and B. Johansson, Phys. Rev. B **78**, 195304 (2008).

[47]M. C. Håkansson, L. S. O. Johansson, C. B. M. Andersson, U. O. Karlsson, L. Ö. Olsson, J. Kanski, L. Ilver, and P. O. Nilsson, Surf. Sci. **374**, 73 (1997).

[48]I. Aureli, V. Corradini, C. Mariani, E. Placidi, F. Arciprete, and A. Balzarotti, Surf. Sci. **576**, 123 (2005).

[49]P. De Padova, P. Perfetti, C. Quaresima, C. Richter, M. Zerrouki, O. Heckmann, V. Ilakovac, and K. Hricovini, Appl. Surf. Sci. **212–213**, 10 (2003).

[50]L. Ö. Olsson, C. B. M. Andersson, M. C. Håkansson, J. Kanski, L. Ilver, and U. O. Karlsson, Phys. Rev. Lett. **76**, 3626 (1996).

[51]C. Ohler, R. Kohleick, A. Förster, and H. Lüth, Phys. Rev. B **50**, 7833 (1994).

[52]M. Noguchi, K. Hirakawa, and T. Ikoma, Phys. Rev. Lett. **66**, 2243 (1991).

[53]J. R. Weber, A. Janotti, and C. G. Van de Walle, Appl. Phys. Lett. **97**, 192106 (2010).